THE JOURNAL OF BIOLOGICAL CHEMISTRY VOL. 282, NO. 31, pp. 22930–22938, August 3, 2007

The Putative Moss 3′-Phosphoadenosine-5′-phosphosulfate Reductase Is a Novel Form of Adenosine-5′-phosphosulfate Reductase without an Iron-Sulfur Cluster*

Received for publication, March 23, 2007, and in revised form, May 18, 2007 Published, JBC Papers in Press, May 22, 2007, DOI 10.1074/jbc.M702522200

Stanislav Kopriva[‡1], **Kai Fritzemeier**[§], **Gertrud Wiedemann**[¶], **and Ralf Reski**[¶]

From the [‡]*Department of Metabolic Biology, John Innes Centre, Norwich NR4 7UH, United Kingdom and the* [§]*Plant Biochemistry and* [¶]*Plant Biotechnology Sections, Faculty of Biology, University of Freiburg, Schaenzlestrasse 1, 79104 Freiburg, Germany*

Sulfate assimilation provides reduced sulfur for synthesis of the amino acids cysteine and methionine and for a range of other metabolites. Sulfate has to be activated prior to reduction by adenylation to adenosine 5′-phosphosulfate (APS). In plants, algae, and many bacteria, this compound is reduced to sulfite by APS reductase (APR); in fungi and some cyanobacteria and γ-proteobacteria, a second activation step, phosphorylation to 3′-phosphoadenosine 5′-phosphosulfate (PAPS), is necessary before reduction to sulfite by PAPS reductase (PAPR). We found previously that the moss *Physcomitrella patens* is unique among these organisms in possessing orthologs of both APR and PAPR genes (Koprivova, A., Meyer, A. J., Schween, G., Herschbach, C., Reski, R., and Kopriva, S. (2002) *J. Biol. Chem.* 277, 32195–32201). To assess the function of the two enzymes, we compared their biochemical properties by analysis of purified recombinant proteins. APR from *Physcomitrella* is very similar to the well characterized APRs from seed plants. On the other hand, we found that the putative PAPR preferentially reduces APS. Sequence analysis, analysis of UV-visible spectra, and determination of iron revealed that this new APR, named PpAPR-B, does not contain the FeS cluster, which was previously believed to determine the substrate specificity of the otherwise relatively similar enzymes. The lack of the FeS cluster in PpAPR-B catalysis is connected with a lower turnover rate but higher stability of the protein. These findings show that APS reduction without the FeS cluster is possible and that plant sulfate assimilation is predominantly dependent on reduction of APS.

Sulfur is essential for life. It is present in the amino acids cysteine and methionine as part of proteins and peptides; in many coenzymes and prosthetic groups, such as FeS centers, thiamine, lipoic acid, etc.; and in a variety of secondary metabolites, *e.g.* glucosinolates and alliins in plants. In these compounds, sulfur is present in the reduced form of organic thiols; however, the major form of sulfur available in nature is sulfate. This has to be reduced and incorporated into organic compounds in the sulfate assimilation pathway, which is present in photosynthetic organisms, fungi, and many bacteria, but not in metazoans and bacteria adapted to a parasitic lifestyle. In the sulfate assimilation pathway, sulfate is taken up into cells by sulfate transporters. Before reduction, it is activated by adenylation to adenosine 5′-phosphosulfate (APS),[2] which is catalyzed by ATP sulfurylase (Fig. 1). APS can be reduced directly to sulfite by APS reductase (APR) or undergo a second activation step, phosphorylation by APS kinase to 3′-phosphoadenosine 5′-phosphosulfate (PAPS). Subsequently, PAPS is reduced by thioredoxin-dependent PAPS reductase (PAPR) to sulfite. Sulfite is further reduced to sulfide by sulfite reductase and incorporated into the amino acid acceptor of *O*-acetylserine (reviewed in Refs. 1 and 2).

APS and PAPS differ only by a single phospho group, similar to NADH and NADPH. Accordingly, APR and PAPR are homologous proteins sharing ~20% identical amino acid residues, including two highly conserved domains, a sulfonucleotide-binding domain, and a catalytic domain containing the active-site cysteine (3, 4). The major difference between the two enzymes is the presence of an iron-sulfur center as a cofactor in APRs (3–8). APRs from plants and green algae also possess a C-terminal domain that functions as a glutaredoxin in the transfer of electrons from glutathione (9, 10). The reaction catalyzed by APR can be divided into three steps. In the first step, APS binds to the protein, and a reductive transfer results in sulfite bound to the active-site cysteine in a stable reaction intermediate (10, 11). In the second step, free sulfite is released by the action of the C-terminal domain in plants or free thioredoxin in bacteria. In the third step, the glutaredoxin active site or thioredoxin is regenerated by reduction with GSH or thioredoxin reductase (10, 11). All available evidence points to the conclusion that the ability to reduce APS is linked to the presence of the iron-sulfur cluster (4). Not only do all confirmed APRs, including dissimilatory APR from sulfate-reducing bacteria, possess the FeS cluster, but when the bifunctional APR/PAPR

* This work was supported by Deutsche Forschungsgemeinschaft Grant KO2065/3 (Research Group FOR 383 "Sulfur Metabolism in Plants: Junction of Basic Metabolic Pathways and Molecular Mechanisms of Stress Resistance"). The costs of publication of this article were defrayed in part by the payment of page charges. This article must therefore be hereby marked "*advertisement*" in accordance with 18 U.S.C. Section 1734 solely to indicate this fact.

[1] To whom correspondence should be addressed. Tel.: 44-1603-450-276; Fax: 44-1603-450-014; E-mail: stanislav.kopriva@bbsrc.ac.uk.

[2] The abbreviations used are: APS, adenosine 5′-phosphosulfate; APR, adenosine-5′-phosphosulfate reductase; PAPS, 3′-phosphoadenosine 5′-phosphosulfate; PAPR, 3′-phosphoadenosine-5′-phosphosulfate reductase; PpAPR and PpAPR-B, *P. patens* 3′-phosphoadenosine-5′-phosphosulfate reductase and homolog, respectively; PpAPR, *P. patens* adenosine-5′-phosphosulfate reductase; GFP, green fluorescent protein; AtAPR, *A. thaliana* adenosine-5′-phosphosulfate reductase; EcPAPR, *E. coli* 3′-phosphoadenosine-5′-phosphosulfate reductase; PaAPR, *P. aeruginosa* adenosine-5′-phosphosulfate reductase.

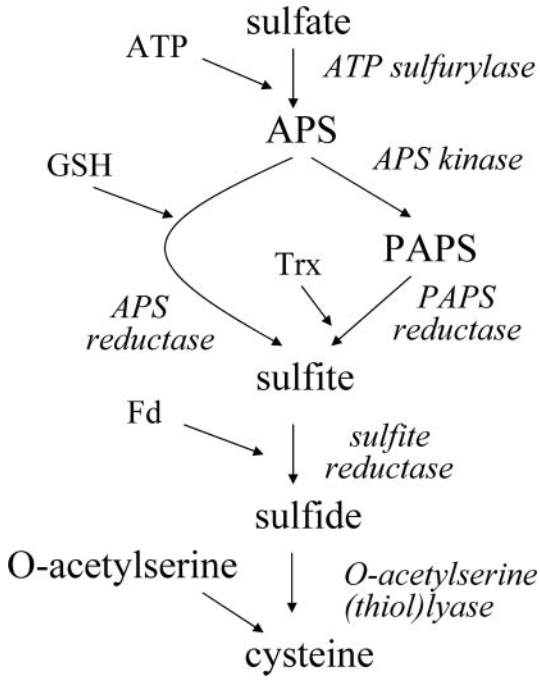

FIGURE 1. **Scheme of the sulfate assimilation pathway in *P. patens*.** *Trx*, thioredoxin; Fd, ferredoxin.

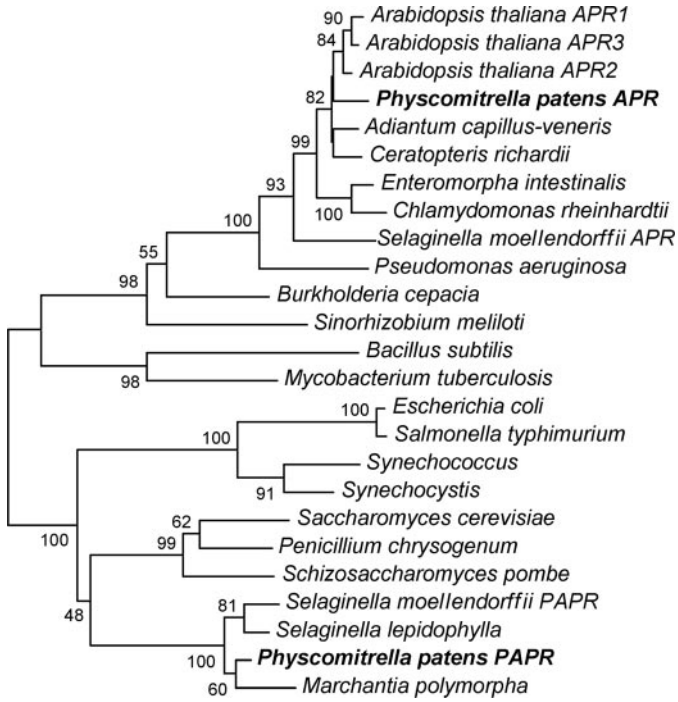

FIGURE 2. **Neighbor-joining tree of APR and PAPR sequences from lower plants.** The amino acid sequences of APRs and PAPRs from lower plants and several typical organisms were retrieved from the GenBank™ Data Bank, aligned using ClustalW, and subjected to phylogenetic analysis with MEGA2 (26) and PhyML (27). Both analyses resulted in trees of the same topology. The *numbers* represent bootstrap support. The *Physcomitrella* sequences are shown in *boldface*.

from *Bacillus subtilis* is deprived of its cofactor, reduction of APS (but not PAPS) is abolished (4, 6, 11). The iron-sulfur cluster is bound to the APR apoenzyme by three or four cysteine residues that are present in the primary sequences as two invariable pairs (3–8). These cysteine pairs thus seem to serve as markers to distinguish between APR and PAPR (3, 4). With one exception, all organisms analyzed to date possess either one or the other enzyme.

The exception is the moss *Physcomitrella patens* (12). In attempts to confirm that APR is the only sulfate-reducing enzyme in plants by analysis of APR knock-outs in *P. patens*, the cDNA for the first putative PAPR from plants was cloned (12). The deduced amino acid sequence of the putative *P. patens* PAPR (PpPAPR) is more similar to the sequences of PAPRs from *Escherichia coli* and fungi than to the sequence of APR from *P. patens* (PpAPR) (Fig. 2). PpPAPR lacks the two cysteine pairs necessary for binding the FeS cluster and does not contain the thioredoxin-like C-terminal extension. However, neither the enzyme activity of the gene product nor its function in *P. patens* sulfate assimilation has been confirmed yet (12). To gain insight into the biological function of the two proteins, we performed biochemical analysis of the recombinant proteins. Here, we provide evidence that, although the protein encoded by the novel cDNA is capable of PAPS reduction, it is much more active with APS as a substrate. Thus, the APS reduction catalyzed by PpPAPR is not dependent on the FeS cluster, and as a consequence, this enzyme should be renamed PpAPR-B.

EXPERIMENTAL PROCEDURES

Plant Material—P. patens (Hedw.) B.S.G. was cultured in liquid or solid Knop medium as described (13). Bioreactor cultures were grown semicontinuously in standard stirred-tank glass bioreactors in Knop medium as described (14).

Localization of PpAPR and PpPAPR—The intracellular localization of PpAPR and PpPAPR was addressed by transient expression of vectors encoding C-terminal green fluorescent protein (GFP) fusion proteins. The complete open reading frames of *PpAPR* and *PpPAPR* were amplified from *P. patens* RNA by reverse transcription-PCR with primers APRlokfw (TCAGATCTATGGCGTTGAAGGTTGCATCAC) and APRlokrev (CTCCCGGGTTGCAATGCTTGCACAAACCCAAG), introducing BglII and SmaI restriction sites, and primers PAPRlokfw (TCGGATCCATGGCGATGGCTATGGCGGAT) and PAPRlokrev (CTCCCGGGTGTTCTACCACCAACGTGAATTCC), adding BamHI and SmaI sites, respectively. The PCR products were cleaved with the corresponding restriction enzymes and ligated into the BglII-SmaI-digested GFP reporter plasmid mAV4 (15). As a control for plastid targeting, pCTP-GFP, corresponding to the mAV4 vector containing the chloroplast transit peptide from *P. patens* FtsZ2-1 (formerly called pFtsZ1-(1–93)-GFP in Ref. 16), was used. The identity of plastids is evident from the red chlorophyll autofluorescence.

The plasmid DNA for transfection was prepared with the QIAfilter plasmid maxi kit (Qiagen Inc.). Protoplasts were transiently transfected with 50 μg of circular plasmid DNA. Isolation and regeneration of protoplasts in the absence of any antibiotic drug were carried out as described previously (17). Six days after transfection, the localization of GFP fluorescence was analyzed in live moss protoplasts by confocal laser scanning microscopy (Leica TCS 4D) using 488 nm excitation and two-channel measurement of emission from 510 to 580 nm (green/GFP) as well as 590 nm (red/chlorophyll).

Overexpression of PpAPR and PpPAPR in E. coli—PpAPR and PpPAPR (12) were produced in *E. coli* using the pET14b expression system and purified to homogeneity by SDS-PAGE with the His·Tag® system (Novagen).

Enzyme Assays—APR and PAPR activities were measured as the production of [^{35}S]sulfite, assayed as acid-volatile radioactivity. The reaction mixture contained 5 μg of recombinant PpPAPR (0.1 μg for measurements with APS) or 4 ng of recombinant PpAPR, 50 mM Tris-HCl (pH 9), 500 mM $MgSO_4$, 5 mM dithioerythritol, 1–200 μM [^{35}S]PAPS (specific activity of 1.67 kBq/nmol; PerkinElmer Life Sciences) or 1–330 μM [^{35}S]APS (synthesized according to Ref. 18), and 5 μg of *E. coli* thioredoxin (Sigma) in a volume of 500 μl and was incubated for 30 min at 37 °C (19). To analyze the pH dependence of the reaction, a series of Tris-HCl buffers with varying pH values was used. For calculation of kinetic parameters, the data were linearized according to the Lineweaver-Burk method. Protein concentrations were routinely estimated according to Bradford (20) using bovine serum albumin as a standard.

Determination of Iron—Iron was quantified spectrophotometrically using tripyridyltriazine (21).

Electronic Spectra—UV-visible spectra were recorded on a Lambda 16 instrument (PerkinElmer Life Sciences) equipped with a temperature-controlled cell compartment.

Bioinformatics—Sequence analysis was performed with the web-based platform Biology WorkBench (workbench.sdsc.edu/). Analysis of the *P. patens* genomic sequence was performed on the COSMOSS homepage (www.cosmoss.org). The subcellular localization of APR and PAPR was analyzed by programs available on-line, *viz.* SherLoc (22), WoLF PSORT (23), TargetP (24) and PA-SUB (25). Phylogenetic analysis was performed on protein sequences aligned by ClustalW with MEGA2 Version 2.1 (26) using the neighbor-joining method and with the web-based tool PhyML (27), resulting in the same tree topology. The protein sequences used for analysis were obtained from the GenBank™ Data Bank as follows: *Arabidopsis thaliana* APR (AtAPR)-1 (NP_192370), AtAPR2 (NP_176409), and AtAPR3 (NP_193930); PpAPR (CAD22096) and PpPAPR (CAD32963); *Adiantum capillus-veneris* (BP918674); *Ceratopteris richardii* (AAT09441); *Enteromorpha intestinalis* (AAC26855); *Chlamydomonas reinhardtii* (AAM18118); *Selaginella moellendorffii* APR and PAPR (obtained from analysis of genomic sequence at moss.nibb.ac.jp/); *Pseudomonas aeruginosa* (NP_250447); *Burkholderia cepacia* (AAD50979); *Sinorhizobium meliloti* (AAD55759); *B. subtilis* (P94498); *Mycobacterium tuberculosis* (P65668); *E. coli* (P17854); *Salmonella typhimurium* (P17853); *Synechococcus* (Q55309); *Synechocystis* (P72794); *Saccharomyces cerevisiae* (P18408); *Penicillium chrysogenum* (AAG24520); *Schizosaccharomyces pombe* (Q10270); *Selaginella lepidophylla* (AAT09442); and *Marchantia polymorpha* (combined from expressed sequence tags BJ859590 and BJ853552). Homology modeling was performed with MODELLER Version 9 and was based on the structures of *E. coli* PAPR (EcPAPR; Protein Data Bank code 1SUR) and *P. aeruginosa* APR (PaAPR; code 2GOY, chain B) (28, 29).

TABLE 1
Prediction of subcellular localization of APR and PAPR
Programs available on-line, *viz.* SherLoc (22), WoLF PSORT (23), TargetP (24), and PA-SUB (25), were used to predict the subcellular localization of APR and PAPR.

	APR	PAPR
SherLoc		
Chloroplast	0.99	0.98
Mitochondria	0.001	0.001
WoLF PSORT		
Chloroplast	14	4
Extracellular		1
TargetP		
Chloroplast	0.650	0.652
Mitochondria	0.025	0.037
Secretory		0.021
Other		0.026
PA-SUB		
Chloroplast	99.793	Not possible

RESULTS

Subcellular Localization of PpAPR and PpPAPR—Physcomitrella is unique in possessing genes homologous to plant APR as well as to bacterial and fungal PAPRs. To obtain a first insight into the biological function of the two proteins, we analyzed their intracellular localization. Plant sulfate assimilation occurs in plastids. When compared with their bacterial counterparts, both PpAPR and PpPAPR contain N-terminal extensions carrying all signs of targeting peptides. Several computer prediction programs uniformly indicated localization of both proteins in plastids with high probability (Table 1). To corroborate the prediction, we created constructs coding for C-terminal fusions of PpAPR and PpPAPR with GFP and transfected *Physcomitrella* protoplasts. Plastid localization of both fusion proteins was confirmed by confocal laser scanning microscopy displaying co-localization of the GFP fluorescence signals with red autofluorescence of chlorophyll (Fig. 3). The same signal distribution was obtained with a control construct encoding GFP fused to the chloroplast-targeting peptide of FtsZ2-1 (16). Interestingly, the distribution of the two enzymes within the moss chloroplasts differed significantly. Whereas the PpPAPR-GFP signal was uniformly distributed within the plastids, PpAPR-GFP fluorescence displayed a spotty pattern (Fig. 3) similar to that described previously for *Physcomitrella* hydroperoxide lyase (30).

Biochemical Properties of PpAPR and PpPAPR—To confirm the sulfonucleotide specificities of the two enzymes, we expressed them in *E. coli* and added an N-terminal His tag for easy subsequent purification. As expected, purified PpAPR was dark yellow in color, similar to recombinant APR from *A. thaliana* or *Lemna minor* (5), whereas PpPAPR was colorless. The UV-visible spectrum of PpAPR was very similar to that of AtAPR2, indicating the presence of an FeS cluster as a cofactor, whereas no indication for the same cofactor was detected in the spectrum of PpPAPR (Fig. 4). These findings were confirmed by iron measurements. Although recombinant PpAPR and AtAPR2 contained 3.2 nmol of iron/nmol of protein, no iron was associated with recombinant PpPAPR (data not shown). On an SDS-polyacrylamide gel, recombinant PpAPR was detectable as a single band of 50 kDa, whereas the molecular mass of PpPAPR was 32 kDa (data not shown).

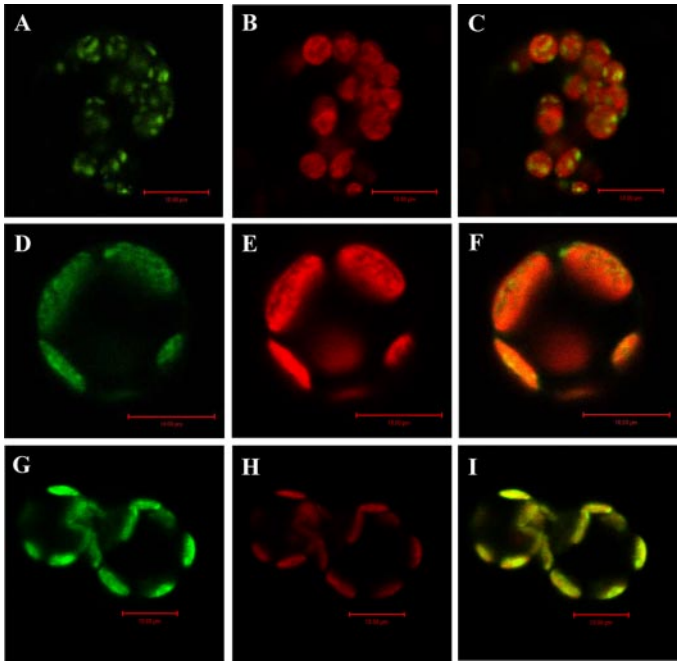

FIGURE 3. **Subcellular localization of PpAPR and PpPAPR.** *P. patens* protoplasts were transfected with expression constructs encoding C-terminal fusions of PpAPR (*A–C*), PpPAPR (*D–F*), and the chloroplast-targeting peptide of FtsZ2-1 (16) (*G–I*). Presented are confocal laser scanning microscopy images 6 days after transfection. *A*, *D*, and *G*, GFP fluorescence; *B*, *E*, and *H*, chlorophyll autofluorescence; *C*, *F*, and *I*, merge of both. *Scale bars* = 10 μm.

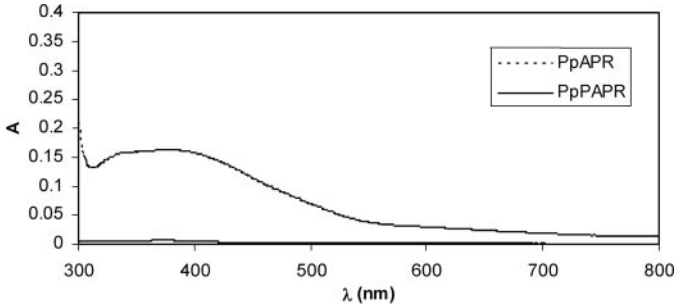

FIGURE 4. **UV-visible spectra of PpAPR and PpPAPR.**

Substrate Specificity of PpAPR and PpPAPR—PpAPR catalyzes the reduction of APS dependent on dithioerythritol or GSH. The properties of the enzyme are similar to those of the well characterized enzyme from *A. thaliana* (4, 5, 10). However, in contrast to AtAPR2, PpAPR was inhibited by APS concentrations >20 μM (Fig. 5*A*). The affinity of both enzymes for APS was very high, with an estimated K_m of 6 μM (Table 2). From this, we calculated a K_{cat} of 37.5 s^{-1} and a K_{cat}/K_m of 6.25 × 10^6 liter M^{-1} s^{-1}. PpPAPR was able to reduce PAPS in a concentration-dependent manner. However, the activity was ~50,000-fold lower than that of PpAPR with APS as a substrate (Fig. 5*B*). The K_m for PAPS was estimated to be 20 μM, which is comparable with that of EcPAPR known from literature (22.5 μM) (31) or determined using bacterial extracts (18 μM) (Fig. 5*B*). Accordingly, the K_{cat} and K_{cat}/K_m values were very low: 7.5 × 10^{-4} s^{-1} and 37.3 liter M^{-1} s^{-1}, respectively. PpAPR did not show any significant activity with PAPS as a substrate (Fig. 5*B*). Surprisingly, however, PpPAPR was much more active with APS as a substrate than with PAPS (Fig. 5*C*). The APS reduction rate increased almost linearly at an APS concentration of up to 100 μM and decreased afterward to ~50% of the maximal value. Compared with PpAPR, the APR activity of PpPAPR was several thousandfold lower at low APS concentrations, but at APS concentrations >50 μM, the difference was only ~200-fold. The K_{cat} of PpPAPR for APS reduction was 0.176 s^{-1}, leading to a K_{cat}/K_m of 3520 liter M^{-1} s^{-1}. EcPAPR was not able to reduce APS at all (Fig. 5*C*). To confirm the substrate specificity of the PpPAPR protein, competition assays with unlabeled APS or PAPS added to the APR or PAPR assays were performed. Whereas the addition of PAPS did not affect APR activity (Fig. 5*D*), the addition of APS inhibited sulfite production from PAPS (Fig. 5*E*). Thus, the putative PAPR from *P. patens*, despite a high similarity to PAPRs from fungi and *E. coli*, catalyzes the reduction of APS. Therefore, this enzyme has been renamed PpAPR-B.

Similar to other plant APRs, PpAPR can use both dithioerythritol and GSH as electron donors. The reaction catalyzed by PpAPR and AtAPR2 was saturated at 4 mM dithioerythritol (Fig. 6*A*). It needed, however, a substantially higher GSH concentration. AtAPR2 activity reached its maximum at 30 mM GSH and was inhibited by higher GSH concentrations (Fig. 6*B*). On the other hand, PpAPR was capable of maximal activity at GSH concentrations of 50 and 100 mM. The maximal reaction velocity of AtAPR2 was ~50% higher with dithioerythritol than with GSH, whereas the activity of PpAPR was identical with both reductants. Because the GSH concentrations necessary for full activity were much higher than the physiological concentrations of 1–5 mM, *in vivo*, APR seems not to function at its full potential.

PpAPR-B (but not PpAPR) was dependent on thioredoxin (Fig. 6*C*). The addition of thioredoxin increased PpAPR-B activity with both substrates, APS and PAPS. The APR activity of PpAPR-B was saturated at 2.5 μM thioredoxin, but PAPS-dependent sulfite production was still increasing. On the other hand, PpAPR activity was not affected by thioredoxin. This was in line with our expectations, as the protein already contains the thioredoxin-like domain necessary for electron transfer (10).

Additional Characteristics of PpAPR and PpAPR-B—The pH dependence of APS reduction by PpAPR was very similar to that of AtAPR2, with low activity at pH ≤ 7 and higher activity at pH ≥ 8.5 (Fig. 7*A*). PpAPR-B activity in terms of APS reduction increased gradually and less markedly with increasing pH. On the other hand, the PAPS-dependent activity of PpAPR-B showed a clear optimum at pH 8 (Fig. 7*B*). To test whether PpAPR or AtAPR might be capable of PAPS reduction at a different pH than in the standard assay, we also measured this reaction at varying pH values. However, the two enzymes did not show any indication of PAPR activity. As a control for PAPR, an extract of *E. coli* was analyzed in the same way and showed a pH optimum between pH 8 and 8.5 with a slower decrease of activity at more alkaline pH (Fig. 7*B*).

Plant APRs are very unstable enzymes because of the rapid loss of their iron-sulfur clusters (5). Indeed, PpAPR and AtAPR2 were completely inactivated after 1 day at −20 °C. In contrast, PpAPR-B retained 30% of its activity after the same storage time (data not shown). When kept at 4 °C, AtAPR2 started to lose activity after 24 h and was completely inactivated

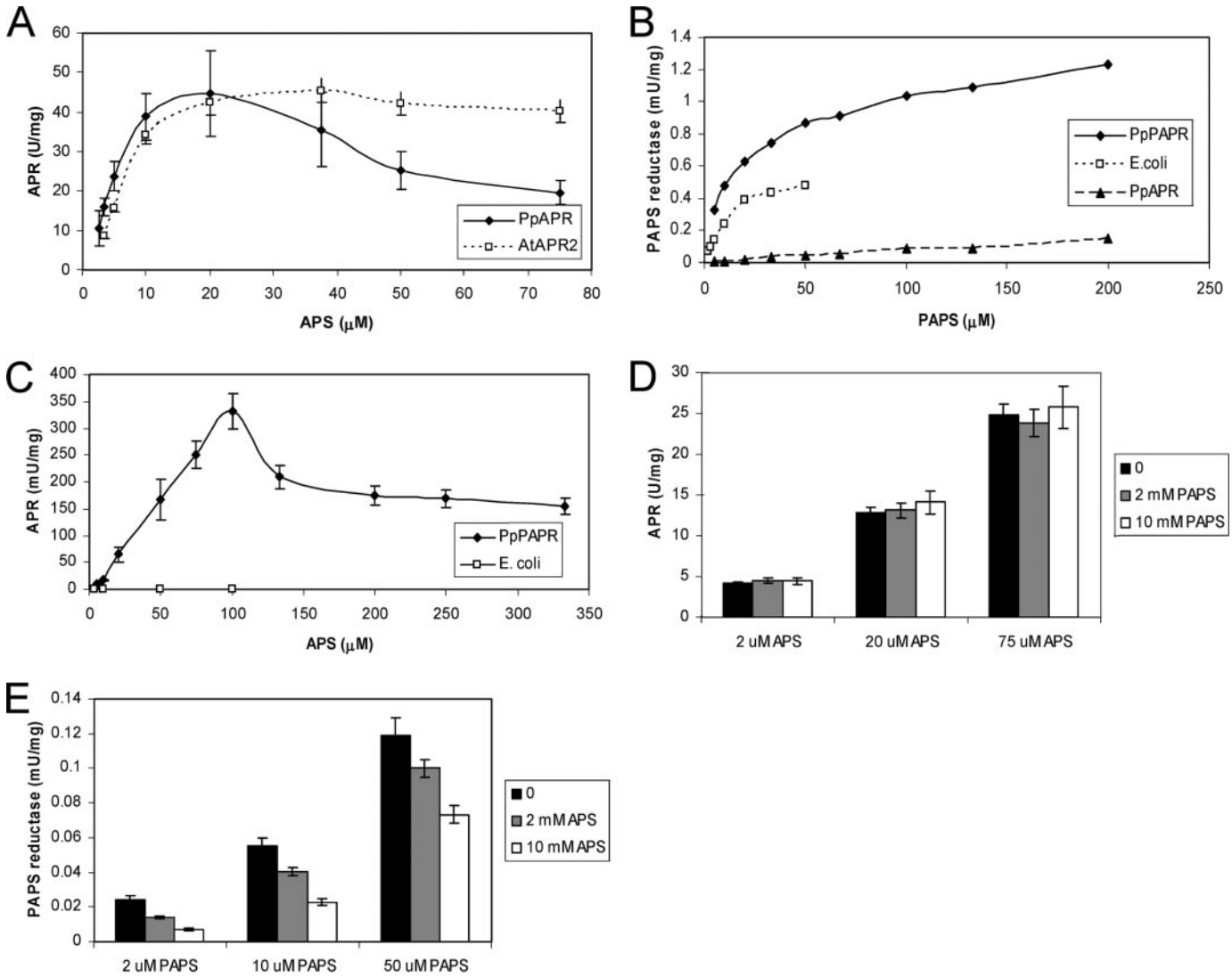

FIGURE 5. **Activity of PpAPR and PpPAPR with APS and PAPS.** *A*, APR activity was measured with purified recombinant PpAPR and AtAPR2 as production of sulfite from varying concentrations of [^{35}S]APS in the presence of dithioerythritol. *B*, PAPR activity was measured with purified recombinant PpAPR and PpPAPR and protein extracts of *E. coli* as production of sulfite from varying concentrations of [^{35}S]PAPS in the presence of dithioerythritol and recombinant thioredoxin from *E. coli*. *C*, APR activity was measured with purified recombinant PpPAPR as production of sulfite from varying concentrations of [^{35}S]APS in the presence of dithioerythritol and recombinant thioredoxin from *E. coli*. *D*, APR activity was measured with purified recombinant PpPAPR as production of sulfite from varying concentrations of [^{35}S]APS in the presence of dithioerythritol, recombinant thioredoxin from *E. coli*, and varying concentrations of PAPS. *E*, PAPR activity was measured with purified recombinant PpPAPR as production of sulfite from varying concentrations of [^{35}S]PAPS in the presence of dithioerythritol, recombinant thioredoxin from *E. coli*, and varying concentrations of APS. The results are presented as the means ± S.D. from measurements of three independent protein isolations.

TABLE 2

Kinetic constants of PpAPR, PpAPR-B, and AtAPR2

APR and PAPR activities were measured with purified recombinant PpAPR, PpPAPR, and AtAPR2 as production of sulfite from varying concentrations of [^{35}S]APS and [^{35}S]PAPS in the presence of dithioerythritol and thioredoxin. The data for EcPAPR are from Ref. 31.

	K_m	V_{max}	K_{cat}	K_{cat}/K_m
	μM	*units/mg*	s^{-1}	*liter* M^{-1} s^{-1}
AtAPR2	6	45	37.5	6,250,000
PpAPR	6	45	37.5	6,250,000
PpAPR-B/APS	50	0.33	0.176	3520
PpAPR-B/PAPS	20	0.0014	0.00075	37
EcPAPR	22.5	6.6	3.5	155,000

after 4 days. PpAPR did not lose any activity for 48 h, but the enzyme was inactivated afterward and retained only ~15% of the initial activity at days 4 and 5. On the other hand, PpAPR-B was stable over 5 days (data not shown). The two APR isoforms of *P. patens* differed also in their temperature dependence. Whereas 37 °C was the optimal temperature for both of them, PpAPR was slightly more active at lower temperature, but was sensitive to high temperature, losing 70% of its activity at 45 °C (data not shown). PpAPR-B and AtAPR2 retained full enzyme activity at 45 °C.

APR activity has been shown previously to be stimulated by sulfate and other salts (32). Congruently, the activities of AtAPR2 and PpAPR were increased by 18- and 24-fold in the presence of 500 mM $MgSO_4$ compared with measurements in 50 mM Tris-HCl, dithioerythritol, and APS without any other salt addition (Fig. 8). PpAPR (but not AtAPR2) was also highly stimulated by $(NH_4)_2SO_4$. The addition of 500 mM $MgCl_2$ and KNO_3 resulted in lower APR activity than without any salt. PpAPR-B was stimulated by all four salts used in the experi-

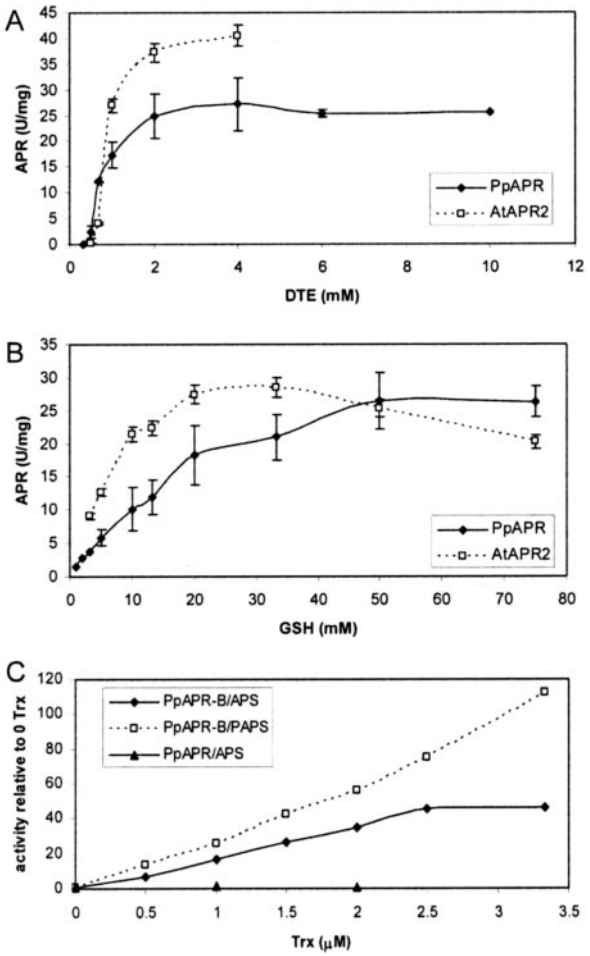

FIGURE 6. **Activity of PpAPR and PpAPR-B with the reductants dithioerythritol and GSH.** *A*, APR activity was measured with purified recombinant PpAPR and AtAPR2 as production of sulfite from 37.5 μM [^{35}S]APS in the presence of varying concentrations of dithioerythritol. *B*, APR activity was measured with purified recombinant PpAPR and AtAPR2 as production of sulfite from 37.5 μM [^{35}S]APS in the presence of varying concentrations of GSH. The results are presented as the means ± S.D. from measurements of three independent protein isolations. *C*, APR or PAPR activity was measured with purified recombinant PpAPR and PpAPR-B as production of sulfite from 37.5 μM [^{35}S]APS or 20 μM [^{35}S]PAPS in the presence of dithioerythritol and varying concentrations of recombinant thioredoxin (*Trx*) from *E. coli*. The activity is presented relative to the activity without thioredoxin. The results are presented as the means from measurements of two independent protein isolations.

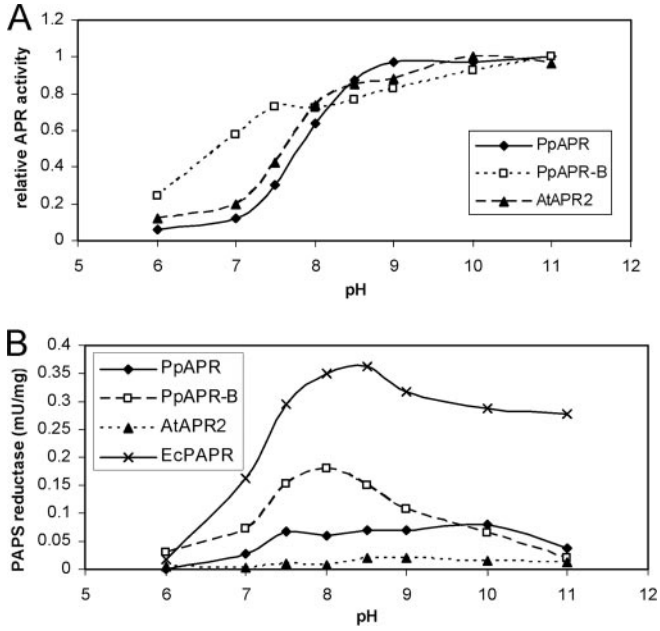

FIGURE 7. **pH dependence of APR and PAPR activities.** *A*, APR activity was measured with purified recombinant PpAPR, PpAPR-B, and AtAPR2 as production of sulfite from 37.5 μM [^{35}S]APS, dithioerythritol, and recombinant thioredoxin from *E. coli* at different pH values. The results are presented relative to activity at the pH optimum. *B*, PAPR activity was measured with purified recombinant PpAPR, PpAPR-B, and AtAPR2 and with extracts of *E. coli* as production of sulfite from 20 μM [^{35}S]PAPS, dithioerythritol, and recombinant thioredoxin from *E. coli* at different pH values.

ment, although the level of induction by sulfate was not as high as for PpAPR (Fig. 8). In contrast, none of the salts at 0.5 M stimulated the activity of EcPAPR.

Modeling of the APS/PAPS-binding Pocket—APS and PAPS differ only by the presence of a phosphate group. According to sequence analysis, PpAPR-B was predicted to catalyze PAPS reduction. However, the enzyme preferentially reacted with APS. Because the crystal structures of EcPAPR and PaAPR are known (28, 29), we aimed to identify which amino acid changes led to the different substrate specificity. Fig. 9 shows the comparison of the sulfonucleotide-binding pockets of PpAPR-B, PaAPR, and EcPAPR with bound substrates. Evidently, the overall structures of the binding sites in all three proteins are very similar. The model predicts a close proximity of Asp^{85} and Arg^{187} of PpAPR-B to the 3′-hydroxyl of ribose carrying the phospho group in PAPS (Fig. 9*A*). A similar configuration with two large and charged amino acid residues (Asp and Gln) is present in the APS-binding pocket of PaAPR (Fig. 9*B*). On the other hand, in EcPAPR, the phosphate seems to be accommodated because of substitutions of Asp^{85} by Gly and Arg^{187} by Leu (Fig. 9*C*).

PpAPR-B Homologs in Other Plant Species—Because the *PpAPR-B* gene has higher sequence similarity to the genes from fungi and bacteria than to those from plants, it was possible to speculate that its presence in *Physcomitrella* is a result of a recent horizontal gene transfer (4). However, expressed sequence tags from *S. lepidophylla* (lycophyte) and *M. polymorpha* (liverwort) encoding *PpAPR-B* orthologs were also found in data bases. More important, the genome of another lycophyte species, *S. moellendorffii*, is being sequenced, and the trace files are available in the public data base. Sequence analysis revealed that *S. moellendorffii* possesses a single copy ortholog of *PpAPR-B* and a single gene for the plant-like APR. The four lower plant PpAPR-B homologs are highly conserved at the amino acid level, and in phylogenetic analysis, they cluster together (Fig. 2), revealing that they have a common evolutionary origin. Indeed, when expressed in *E. coli*, *S. lepidophylla* APR-B was active as APR, similar to PpAPR-B (data not shown). Therefore, it seems that, sometime during evolution, the substrate specificity of the original PAPR was altered to APS. Because lycophytes are already vascular plants, the common ancestor of bryophytes, liverworts, and vascular plants had to possess both genes. Interestingly, however, APR from *S. moellendorffii* does not possess the invariant cysteine residue in the active center, which is conserved among all APRs and PAPRs. Because this cysteine is essential for catalysis, the gene product will most probably not be functional. This and other

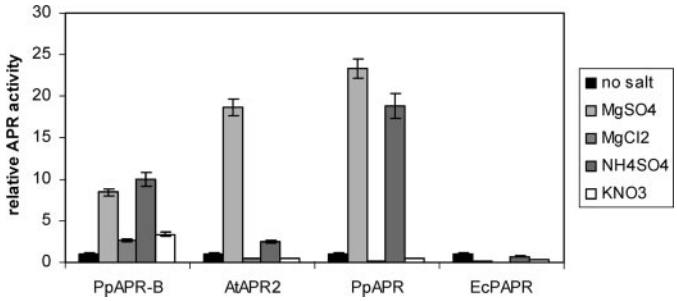

FIGURE 8. **Effect of salts on APR activity.** APR activity was measured with purified recombinant PpAPR, PpAPR-B, and AtAPR2 in 50 mM Tris-HCl (pH 9), 5 mM dithioerythritol, and 37.5 μM APS (100 μM APS and 3 μM *E. coli* thioredoxin for PpAPR-B) with additions of 500 mM salts as indicated. PAPR was measured with protein extracts from *E. coli* under the same conditions, substituting APS for 20 μM PAPS in the presence of 3 μM thioredoxin. The results are presented relative to activity without salt addition as the means ± S.D. from measurements of three independent protein isolations.

nucleotide substitutions result in branching of the *S. moellendorffii* APR before the node separating plants and green algae (Fig. 2).

DISCUSSION

It has been generally adopted that PAPRs exist in fungi and bacteria only, whereas plants reduce APS directly (1, 3). The cloning of a cDNA encoding a putative PAPR in *P. patens* already challenged this view. However, because no enzyme activity had been measured, the significance of this finding was limited (12). The putative PAPR from *P. patens* (PpAPR-B) is in many respects similar to bacterial and fungal PAPRs. Its amino acid sequence is 26.6 and 25.7% identical to PAPRs from *E. coli* and *S. cerevisiae*, but only 20.6 and 20.3% identical to APRs from *A. thaliana* and *P. patens*. In the phylogenetic analysis, it clearly clusters with other PAPRs from bacteria and fungi (Fig. 2). More important, it does not possess the two Cys pairs that bind the iron-sulfur cluster, which have been considered as markers for APS-dependent reduction (3). In addition, the enzyme does not possess the thioredoxin-like domain found in plant APRs. Therefore, the enzyme was clearly expected to catalyze thioredoxin-dependent sulfite production from PAPS. Indeed, sulfite production from PAPS dependent on the substrate concentration was measured (Fig. 5*B*), and the reaction was strongly stimulated by thioredoxin (Fig. 6*C*). The affinity for PAPS (K_m = 20 μM) (Table 1) was highly comparable with that of the *E. coli* and yeast enzymes, with K_m values of 22.5 and 19 μM, respectively (19, 31). The reaction velocity was similar to that of yeast PAPR (19). The V_{max} of the yeast enzyme was 4–7 milliunits/mg using a yeast thioredoxin, but dropped to 0.4 milliunits/mg when heterologous thioredoxin from *E. coli* was used (19). The latter value is even lower than the V_{max} of PpAPR-B in the PAPR reaction (1.4 milliunits/mg), which was also determined in a heterologous system using *E. coli* thioredoxin. Therefore, it can be expected that the reaction velocity with homologous thioredoxin will be ~10-fold higher, in the range of 14 milliunits/mg. In contrast, the V_{max} of EcPAPR is ~500-fold higher (5.1–6.6 units/mg). PpAPR-B thus indeed seems to act as a PAPR.

However, testing the ability of PpAPR-B to catalyze APS reduction revealed that, with this substrate, the enzyme is much more active. Sulfite production from APS was ~50,000-fold higher than that from PAPS and was also dependent on thioredoxin. In competition assays in which unlabeled APS or PAPS was added to radioactive PAPS or APS, respectively, PAPS was not able to compete with [^{35}S]APS and to reduce the APS reduction rate. On the other hand, unlabeled APS reduced the production of [^{35}S]sulfite from [^{35}S]PAPS, showing that the enzyme acts primarily as an APR. Among the plant APRs, PpAPR-B is the only bifunctional one because other tested enzymes (PpAPR and AtAPR2) were not capable of PAPS reduction. Dual substrate specificity for both APS and PAPS was described, however, for the CysH protein from *B. subtilis* (6). In contrast to PpAPR-B, which catalyzes APS reduction ~100 times more efficiently (*cf.* K_{cat}/K_m for APS and PAPS reduction), only an ~5-fold difference in K_{cat}/K_m between the two substrates was found for the *B. subtilis* enzyme. The K_{cat} was comparable between APS and PAPS reduction, and so the difference in efficiency was driven by a higher affinity of the protein for PAPS (6). The PAPR activity of PpAPR-B thus seems to be too low compared with the rate of APS reduction to merit the enzyme to be called bifunctional. The enzyme was thus named PpAPR-B to avoid confusion with the numbering of APR isoforms of higher plants, *e.g.* APR1, APR2, and APR3 of *A. thaliana*.

These findings thus contradict the accepted view that APR activity is linked to the presence of an iron-sulfur cluster (3, 11, 29). Indeed, all sulfonucleotide reductases using APS analyzed to date possess the cofactor, including dissimilatory APR, plant APR with the thioredoxin-like domain, and bacterial APR. In contrast, no FeS clusters were found in PAPRs from fungi, yeast, and enteric bacteria, except for the bifunctional enzyme from *B. subtilis* (3, 6–8, 11, 29). However, even in *B. subtilis*, the APS reduction is strictly dependent on the presence of the cluster, whereas the enzyme deprived of the cofactor is still capable of PAPS reduction (6). PpAPR-B does not possess the FeS cluster, as demonstrated by UV-visible spectroscopy, and consequently, no iron bound to the protein could be measured. The enzyme thus represents a new form of APR independent of the FeS chemistry. The cost of the lack of cofactor is substantial, as on the basis of the K_{cat}/K_m, PpAPR-B is 1770-fold less efficient than PpAPR. At physiological APS concentrations <10 μM, the reaction velocity of PpAPR is 2500 times higher than that of PpAPR-B. Why there is such a difference in activity between the two proteins is not obvious. The low reaction velocity of PpAPR-B explains, however, why we were not able to detect APR or PAPR activity in crude extracts of moss knock-outs in PpAPR (12). In addition, the two isoforms differ in their optimal reaction conditions and in that PpAPR-B requires the addition of thioredoxin. If both enzymes are present at the same level in moss, the *in vitro* activity of PpAPR-B contributes <0.1% of the total activity, which is under the detection limit of the assay. Despite the much lower reaction velocity, however, PpAPR-B is clearly able to compensate for the lack of APR in Δ*APR* (PpAPR knock-out) plants *in vivo* (12).

What could be the evolutionary advantages of this novel APR isoform? An additional PAPR could be able to salvage sulfur from PAPS otherwise lost in secondary metabolism. As PpAPR-B is also capable of this reaction, this could be one of the

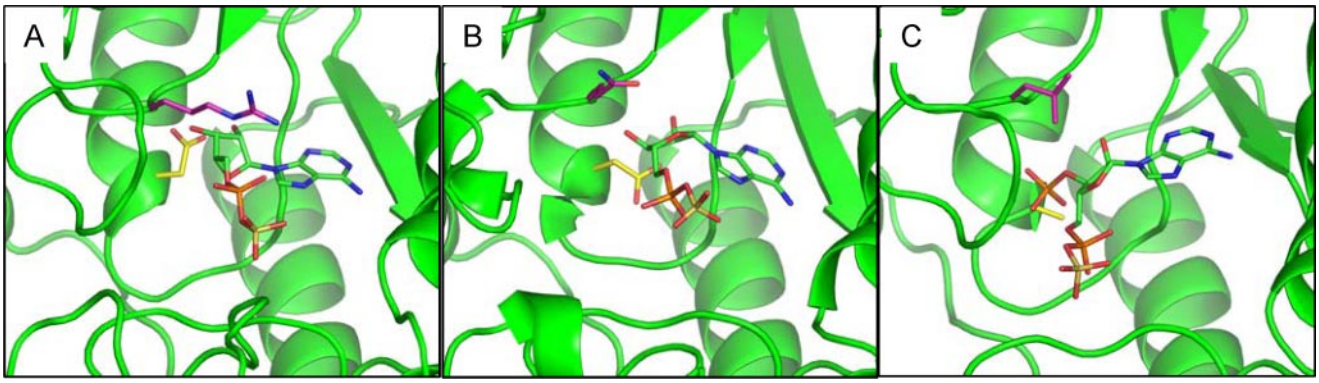

FIGURE 9. **Homology modeling of the sulfonucleotide-binding pocket.** The sulfonucleotide-binding pocket was modeled with MODELLER Version 9 based on the structures of EcPAPR (Protein Data Bank code 1SUR) and PaAPR (code 2GOY, chain B) (28, 29). *A*, PpAPR-B with bound APS; *B*, EcPAPR with bound PAPS; *C*, PaAPR with bound APS. Asp^{85} of PpAPR-B and the corresponding residues Asp and Gly are shown in *yellow*, and Arg^{187} of PpAPR-B and Gln and Leu of PaAPR and EcPAPR are colored *magenta*.

potential benefits to retain an alternative enzyme to PpAPR. The major advantage of PpAPR-B compared with PpAPR is, however, its high stability. Plant APRs are rapidly inactivated and have a quick turnover. Possessing a second, stable isoform of the enzyme lowers the need for a constant replacement of the enzyme. In addition, the new isoform of APR does not need the FeS cluster and thus is advantageous under iron-limiting conditions, *e.g.* in aquatic habitats of the mosses. This could also be achieved with PAPR, but the consequence of the change in the active center is saving one ATP/molecule of APS reduced by the new enzyme and thus a substantial saving of energy. Consequently, PpAPR-B contributes to the huge pool of metabolic moss genes that are absent in seed plants (33). However, it seems that APS reduction is the only route of sulfate assimilation in both seed and basal plants.

As PpAPR-B evidently evolved from a PAPR by changing the substrate-binding site, it was interesting to find out which amino acid changes led to the alteration of substrate specificity. The two sulfonucleotides APS and PAPS differ only by the presence of a phosphate group modifying the 3′-residue of ribose. A similar modification distinguishes NAD^+ and $NADP^+$ dinucleotide cofactors. A great effort was put into understanding the differences in the binding of the two cofactors and engineering the corresponding binding pockets (34, 35). Comparison of the crystal structures of PaAPR and EcPAPR suggested that the substrate specificity for APS is determined by Glu^{65} and Asp^{66} of PpAPR (29). These residues are invariant in >30 plant APRs and are present in all confirmed bacterial APRs. The bifunctional APR/PAPR from *B. subtilis* has Gly in place of Asp^{66}, probably to enable binding of both substrates. Some other bacterial enzymes that possess the two Cys pairs and were therefore assumed to be APRs possess Ser instead of Asp^{66} or Asp instead of Glu^{65}. EcPAPR possesses two small amino acids in place of Glu^{65} and Asp^{66}, *i.e.* Gln and Ala, respectively. The sequence of PpAPR-B and the orthologs in *Selaginella* and *Marchantia* is Gly^{84}-Asp^{85}. Therefore, these enzymes are more similar to the plant/bacterial APRs than to PAPRs. Homology modeling confirmed the higher similarity of the binding pocket of PpAPR-B to that of PaAPR compared with EcPAPR. It also revealed a close proximity of Asp^{85} to the 3′-hydroxyl of ribose, which may be responsible for the alteration of the binding pocket to accommodate APS instead of PAPS. However, a second residue, Arg^{187}, also seems to interact with the 3′-OH group. A small uncharged amino acid (Leu) is at this position in most bacterial PAPRs, so it seems that also this residue is involved in the determination of substrate specificity. Site-directed mutagenesis experiments will be necessary to show whether these amino acid residues are indeed implicated in the distinction between APR and PAPR. The change in substrate specificity resulted, however, in a reduction in catalytic efficiency compared with EcPAPR, which has a 50-fold higher K_{cat}/K_m compared with PpAPR-B. Our current findings thus show that APS reduction without the FeS cluster is possible and that the usefulness of the two cysteine pairs as markers to distinguish APS- and PAPS-dependent sulfate reduction has to be re-appraised.

Acknowledgments—We thank Andreas Zimmer for introduction to programs on the prediction of subcellular localization of proteins, Louis Gremillon for help with confocal microscopy, Michael McManus for critical reading of the manuscript, and Anne Katrin Prowse for help with editing the manuscript.

REFERENCES

1. Leustek, T., Martin, M. N., Bick, J. A., and Davies, J. P. (2000) *Annu. Rev. Plant Physiol. Plant Mol. Biol.* **51,** 141–165
2. Kopriva, S. (2006) *Ann. Bot.* **97,** 479–495
3. Kopriva, S., Büchert, T., Fritz, G., Suter, M., Benda, R., Schünemann, V., Koprivova, A., Schürmann, P., Trautwein, A. X., Kroneck, P. M. H., and Brunold, C. (2002) *J. Biol. Chem.* **277,** 21786–21791
4. Kopriva, S., and Koprivova, A. (2004) *J. Exp. Bot.* **55,** 1775–1783
5. Kopriva, S., Büchert, T., Fritz, G., Suter, M., Weber, M., Benda, R., Schaller, J., Feller, U., Schürmann, P., Schünemann, V., Trautwein, A. X., Kroneck, P. M., and Brunold, C. (2001) *J. Biol. Chem.* **276,** 42881–42886
6. Berndt, C., Lillig, C. H., Wollenberg, M., Bill, E., Mansilla, M. C., de Mendoza, D., Seidler, A., and Schwenn, J. D. (2004) *J. Biol. Chem.* **279,** 7850–7855
7. Kim, S. K., Rahman, A., Bick, J. A., Conover, R. C., Johnson, M. K., Mason, J. T., Hirasawa, M., Leustek, T., and Knaff, D. B. (2004) *Biochemistry* **43,** 13478–13486
8. Carroll, K. S., Gao, H., Chen, H., Leary, J. A., and Bertozzi, C. R. (2005) *Biochemistry* **44,** 14647–14657
9. Bick, J. A., Aslund, F., Chen, Y., and Leustek, T. (1998) *Proc. Natl. Acad. Sci. U. S. A.* **95,** 8404–8409

10. Weber, M., Suter, M., Brunold, C., and Kopriva, S. (2000) *Eur. J. Biochem.* **267,** 3647–3653
11. Carroll, K. S., Gao, H., Chen, H., Stout, C. D., Leary, J. A., and Bertozzi, C. R. (2005) *PLoS Biol.* **3,** e250
12. Koprivova, A., Meyer, A. J., Schween, G., Herschbach, C., Reski, R., and Kopriva, S. (2002) *J. Biol. Chem.* **277,** 32195–32201
13. Reski, R., and Abel, W. O. (1985) *Planta* **165,** 354–358
14. Hohe, A., Decker, E. L., Gorr, G., Schween, G., and Reski, R. (2002) *Plant Cell Rep.* **20,** 1135–1140
15. Kircher, S., Kozma-Bognar, L., Kim, L., Adam, E., Harter, K., Schäfer, E., and Nagy, F. (1999) *Plant Cell* **11,** 1445–1456
16. Kiessling, J., Kruse, S., Rensing, S. A., Harter, K., Decker, E. L., and Reski, R. (2000) *J. Cell Biol.* **151,** 945–950
17. Rother, S., Hadeler, B., Orsini, J. M., Abel, W. O., and Reski, R. (1994) *J. Plant Physiol.* **143,** 72–77
18. Li, J., and Schiff, J. A. (1991) *Biochem. J.* **274,** 355–360
19. Schwenn, J. D., Krone, F. A., and Husmann, K. (1988) *Arch. Microbiol.* **150,** 313–319
20. Bradford, M. M. (1976) *Anal. Biochem.* **72,** 248–254
21. Fischer, D. S., and Price, D. C. (1964) *Clin. Chem.* **10,** 21–31
22. Höglund, A., Blum, T., Brady, S., Dönnes, P., Miguel, J. S., Rocheford, M., Kohlbacher, O., and Shatkay, H. (2006) *Pac. Symp. Biocomput.* **11,** 16–27
23. Horton, P., Park, K.-J., Obayashi, T., and Nakai, K. (2006) in *Proceedings of 4th Asia-Pacific Bioinformatics Conference, Taipei, Taiwan, February 13–16, 2006* (Jiang, T., Yang, U.-C., Chen, Y.-P. P., and Wong, L., eds) pp. 39–48, Imperial College Press, London
24. Emanuelsson, O., Nielsen, H., Brunak, S., and von Heijne, G. (2000) *J. Mol. Biol.* **300,** 1005–1016
25. Lu, Z., Szafron, D., Greiner, R., Lu, P., Wishart, D. S., Poulin, B., Anvik, J., Macdonell, C., and Eisner, R. (2004) *Bioinformatics* (*Oxf.*) **20,** 547–556
26. Kumar, S., Tamura, K., Jakobsen, I. B., and Nei, M. (2001) *Bioinformatics* (*Oxf.*) **17,** 1244–1245
27. Guindon, S., Lethiec, F., Duroux, P., and Gascuel, O. (2005) *Nucleic Acids Res.* **33,** 557–559
28. Savage, H., Montoya, G., Svensson, C., Schwenn, J. D., and Sinning, I. (1997) *Structure* (*Camb.*) **5,** 895–906
29. Chartron, J., Carroll, K. S., Shiau, C., Gao, H., Leary, J. A., Bertozzi, C. R., and Stout, C. D. (2006) *J. Mol. Biol.* **364,** 152–169
30. Stumpe, M., Bode, J., Göbel, C., Wichard, T., Schaaf, A., Frank, W., Frank, M., Reski, R., Pohnert, G., and Feussner, I. (2006) *Biochim. Biophys. Acta* **1761,** 301–312
31. Lillig, C. H., Prior, A., Schwenn, J. D., Aslund, F., Ritz, D., Vlamis-Gardikas, A., and Holmgren, A. (1999) *J. Biol. Chem.* **274,** 7695–7698
32. Kim, S. K., Gomes, V., Gao, Y., Chandramouli, K., Johnson, M. K., Knaff, D. B., and Leustek, T. (2007) *Biochemistry* **46,** 591–601
33. Lang, D., Eisinger, J., Reski, R., and Rensing, S. A. (2005) *Plant Biol.* **7,** 238–250
34. Tomita, T., Kuzuyama, T., and Nishiyama, M. (2006) *Biosci. Biotechnol. Biochem.* **70,** 2230–2235
35. Penning, T. M., and Jez, J. M. (2001) *Chem. Rev.* **101,** 3027–3046